DOI: 10.1002/cctc.201500234

Controlling the Course of a Two-Way Switchable Pd-Catalyzed Process by means of Empirical Multivariate Models

Alexander H. Sandtorv and Hans-René Bjørsvik*[a]

A two-way switchable Pd-catalyzed process that can pursue two different mechanisms, namely hydro- and methoxy-deiodination was discovered, developed, and optimized by means of statistical experimental design, multivariate modelling, and response surface methodology. The investigation revealed that the two-way switchable process might be controlled either by ligand alone, or by ligand and other process variables in combination. The present study represents the first example of a catalytic system that provides either hydro- or methoxy-deiodination selectively by simply fine-tuning the experimental variables.

Introduction

Hydrodehalogenation is an essential transformation in organic synthesis.[1] In this context, palladium has been shown to be an efficient catalyst,[2] and several variations have been disclosed recently.[3] If an alcohol is present in the reaction mixture, a competitive *ipso*-substitution-type dehalogenation process can take place, a coupling between the aryl halide and the alcohol to provide an alkoxydehalogenation product.[4] Diverse approaches have been disclosed for pursuing alkoxydehalogenation including treatment with alkoxide,[5] Cu-catalyzed reactions,[6] Ullmann-type coupling reactions,[7,8] and Pd-catalyzed coupling processes.[9,10]

A general mechanism that includes both the hydrodeiodination and methoxydeiodination pathways is outlined in Scheme 1. The β-hydride elimination step (e) determines the main product distribution between alkyl aryl ether (**1**) or aryl (**2**). The common strategy to control the selectivity of this step has been ligand design and engineering with the aim of improving the selectivity of the C–O coupling.[4,10] Sophisticated and dedicated catalytic systems have been synthesized for the combined goal of high selectivity and yield.

In such cases, tuning of the process, or experimental variables has in general been treated very superficially or by the obscure and incomplete OVAT (one-variable-at-a-time) strategy[12] in attempts to optimize the process.

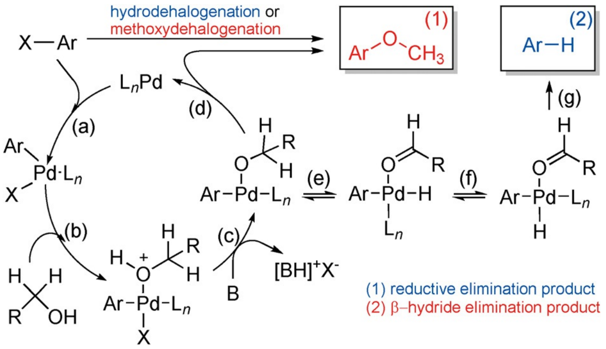

Scheme 1. A general catalytic process proceeding through a hydrodeiodination (X = I) or a methoxydeiodination (R = H) mechanism. Step (a) oxidative addition, step (b) coordination of the alcohol reagent to Pd, step (c) deprotonation by means of base B,[11] step (d) reductive elimination producing the Ar–OR ether, step (e) β-hydride elimination, step (f) isomerization, and step (g) reductive elimination affording the hydrodehalogenated product Ar–H.

Recently, we revealed a switchable Pd-catalyzed process that could operate either as a Suzuki coupling reaction or as a hydrodeiodination reaction working on diiodoimidazoles in the absence of a base.[13] The attained results and potential of this process encouraged us to undertake the investigation disclosed herein, which includes the exploration of the general validity and scope of the method, exploiting haloarenes instead of diiodoimidazoles as substrates. Owing to the basic chemical character, we realized that this investigation was a multivariate challenge, which could only be solved by means of statistical experimental design,[14] multivariate regression,[15] and/or other methods for multivariate data analysis.[16]

Results and Discussion

Pre-experimental design

To obtain an outline of the present multivariate challenge, a pre-experimental design study was performed. Each experi-

---

[a] Dr. A. H. Sandtorv, Prof. Dr. H.-R. Bjørsvik
Department of Chemistry
University of Bergen
Allégaten 41, B-5007 Bergen (Norway)
Fax: (+47) 55-58-94-90
E-mail: hans.bjorsvik@kj.uib.no

Supporting Information for this article is available on the WWW under http://dx.doi.org/10.1002/cctc.201500234.

This publication is part of a Special Issue on Palladium Catalysis. To view the complete issue, visit:
http://onlinelibrary.wiley.com/doi/10.1002/cctc.v7.14/issuetoc

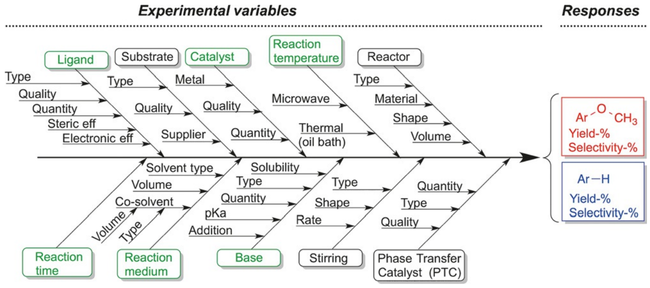

Figure 1. Ishikawa cause-and-effect diagram—mapping of the experimental variables for the two Pd-catalyzed processes hydrodeiodination and methoxydeiodination.

mental variable that was identified was successively included in an Ishikawa cause-and-effect diagram,[17] as shown in Figure 1.

After a review of the process, we came to the conclusion that ten different experimental variables could potentially influence both the performance of the reaction and the direction of the two-way switchable process.

Six of these experimental variables (displayed in green in the Ishikawa diagram of Figure 1) were chosen for further investigation (see the Supporting Information for a discussion of these variables). The other variables were kept at fixed, but carefully designated experimental levels.

Introductory experiments

At the outset, 3-iodo-4-nitrotoluene (**1a**) was used as a model substrate. A series of screening experiments (System I, Scheme 2) were performed to investigate variations of the catalytic system and the influence of various solvents. However, a maximum yield of only ≈3% of the hydrodeiodinated product **2a** was obtained in this screening study.

Further screening included a base (System II, Scheme 2), and revealed that the presence of a base was essential for the hydrodeiodination reaction (see the Supporting Information for details). We also obtained the methoxydeiodinated compound **3a**, a product that was not observed during our previous study.[13] From this investigation, we identified KOH as the optimal base.

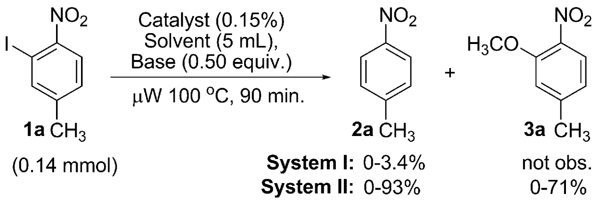

System I

Solvent	MeOH, iso-PrOH, Toluene, DMF, THF
Base	no base
Catalyst	XPhos, $Pd(OAc)_2$, $Pd(OAc)_2$+XPhos, NHC-1, NHC-2

System II

Solvent	Toluene, THF, diglyme, MeOH, MeOH/H_2O
Base	K_2HPO_4, Na_2CO_3, $NaHCO_3$, KH_2PO_4, NH_4HPO_4, KOH, NaOAc, NEt_3
Catalyst	$Pd(OAc)_2$/XPhos

Scheme 2. System I: Introductory screening experiments including variation of solvent and Pd catalyst. System II: Screening of the solvents and bases on the Pd-catalyzed *ipso*-substitution-type dehalogenation processes.

The quantity of the base influenced the reaction performance and KOH provided the highest yields of products **2a** and **3a** (Figure 2a). Furthermore, we discovered that a reaction medium composed of methanol, with or without water as a cosolvent, demonstrated a substantial effect on the reaction outcome; leading to either **2a** or **3a** (see Figure 2b). Increased quantities of water in the reaction medium completely suppressed the methoxydeiodination reaction.

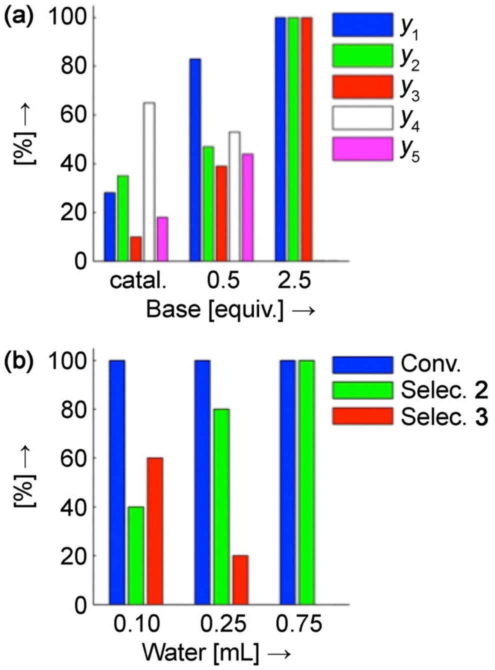

Figure 2. a) Investigation of the effect of base on the *ipso*-type-substitution/dehydrogenation processes. y_1 = conversion based on starting material **1a**, y_2 = selectivity towards the hydrodehalogenation product **2a**, y_3 = yield of the hydrodehalogenation product **2a**, y_4 = selectivity towards the product **3a**, y_5 = yield of methoxydehalogenation product **2a**. All responses were measured by GC–MS. b) Influence of water as cosolvent in methanol as reaction medium. General procedure: 3-nitro-4-iodotoluene **1a** (0.19 mmol), ligand **L3** (0.15 mol%) and KOH [for (a) as described and for (b) 0.5 equiv.], Degassed methanol (5 mL) and $Pd(OAc)_2$ (0.15 mol%), 100 °C for 90 min. Analyzed by GC–MS. See the Supporting Information for details.

We also examined the manner in which the base should be added to the reaction mixture. Addition of KOH as a solid or in solution resulted in a noticeable effect on the reaction yield. The reaction profiles of the hydrodeiodination and methoxydeiodination under these different addition protocols are shown in Figure 3. The reaction profiles clearly show that the methoxydeiodination product **3b** degrades when the reaction time is longer than 100 min. Furthermore, when KOH was added as a solution, there was a noticeable increase in the yield of both products compared to when KOH was added as a solid. We attribute this effect to the fact that KOH is a highly hygroscopic substance and the solid base had absorbed some water.

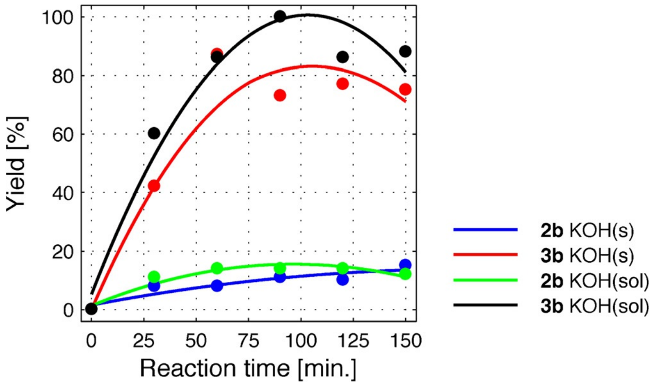

Figure 3. Reaction profile for the hydrodeiodination/methoxydeiodination reaction with KOH added either as a solid or as a solution.

Ligand screening

A ligand screening, including a test library composed of twelve phosphorous ligands (Figure 4) with different steric and electronic properties, was investigated. An alternative and more exhaustive ligand screening could have been carried out by using a multivariate approach, namely by performing a principal component analysis[16] of the physical, chemical, and structural properties of a larger ligand library and selecting a subset from this.[18] However, such an approach would have been laborious and far outside the scope of this study; therefore, we decided to perform a simple experimental screening of a ligand library.

The deactivated iodoarene **1 b** (Table 1) and the activated iodoarene **1 c** (Table 2) were used as model substrates.

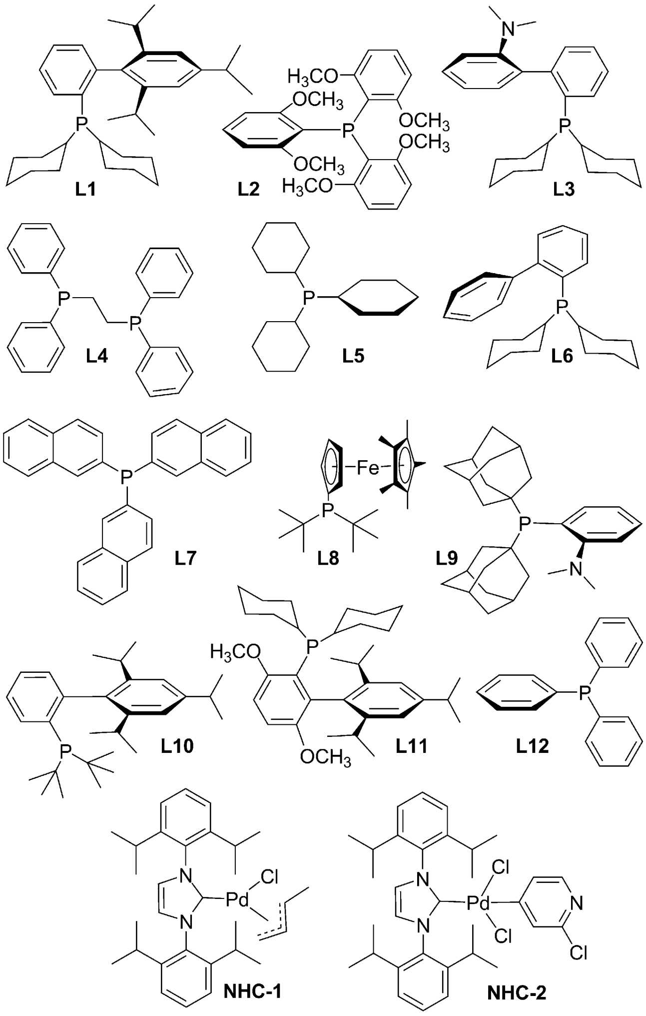

Figure 4. Phosphine ligands and Pd–NHC catalysts.

Table 1. Investigation of the *ipso*-type-substitution deiodination reaction with a deactivated arene.

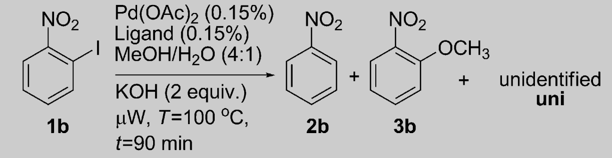

Entry	Ligand	Conv. [%]	Response[a] Sel. **2 b** [%]	Sel. **3 b** [%]	Sel. **uni** [%]
1	**L1**	42	54	46	–
2	**L2**	35	65	35	–
3	**L3**	86	32	68	–
4	**L4**	100	100	0	–
5	**L5**	33	72	15	13
6	**L6**	69	41	59	–
7	**L7**	25	55	45	–
8	**L8**	100	87	10	3
9	**L9**	27	60	40	–
10	**L10**	39	78	11	11
11	**L11**	28	55	45	–
12	**L12**	25	55	45	–
13	no ligand	21	57	20	23

[a] Conv. = Conversion based on substrate **1 b**. Sel. **2 b** = Selectivity towards product **2 b**. Sel. **3 b** = Selectivity towards product **3 b**. Sel. **uni** = Selectivity towards an unidentified byproduct. Responses were measured by GC.

The attempt to perform the hydrodeionation of the deactivated arene **1 b**, provided the expected product **2 b** with selectivity in the range of 41–100% by using the ligands **L1**–**L12**. Furthermore, for a few of the ligands the methoxydeiodinated product **3 b** was produced with selectivities in the range of 10–68% (Table 1). The activated arene **1 c** provided only small quantities of the hydrodeiodinated product **2 c**. An Ullmann-type reaction took place to provide biphenyl **4** (13–17%) when the ligands **L6** or **L8** were used. These experiments show that the electronic structure of the arene substrate was imperative for the performance and success of the studied switchable two-way process (hydrodeiodination and methoxydeiodination), and that arenes elaborated with electron-donating groups were poor substrates.

Statistical experimental design[14] and modelling[15]

Based on the results from the experimental screening described above, we decided to continue the investigation by

Table 2. Investigation of the *ipso*-type-substitution deiodination reaction with an activated arene.

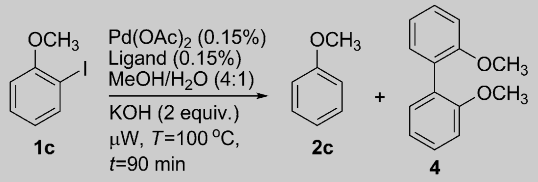

1c **2c** **4**

Entry	Ligand	Conv. [%]	Response[a] Sel. **2c** [%]	Sel. **4** [%]
1	**L1**	0	–	–
2	**L2**	0	–	–
3	**L3**	0	–	–
4	**L4**	0	–	–
5	**L5**	0	–	–
6	**L6**	17	0	100
7	**L7**	0	–	–
8	**L8**	13	0	100
9	**L9**	0	–	–
10	**L10**	5	100	–
11	**L11**	20	100	–
12	**L12**	22	100	–
13	no ligand	26	100	–

[a] Conv. = Conversion based on substrate **1c**. Sel. **2c** = Selectivity towards product **2c**. Sel. **4** = Selectivity towards product **4**. Responses were measured by GC.

using a small sub-set of the P ligands (**L3**, **L4**, and **L6**, Figure 2) for further reaction discovery. In addition to the notable effect of the catalytic system, it was evident that changing the experimental conditions significantly affected both the performance and outcome of the Pd-catalyzed processes. The investigation was continued by using a full factorial design,[19] including some experiments in the center of the experimental domain ($2^k+c=2^4+2=18$). This design included the following experimental variables: x_1 = reaction temperature [°C], x_2 = volume of cosolvent [mL], x_3 = volume of solvent [mL], and x_4 = quantity of base [equiv.]. The design matrix $\mathbf{D}_{\mathrm{FFD}}$ is provided in standard order[20] (Table 3, entries 1–18), but was performed in random order in the laboratory. To facilitate the calculation of the regression coefficients, Equation (1), the experimental variables x_1,.., x_4 were scaled according to Equation (2).

$$y=f(x_1,x_2,x_3,x_4)=\beta_0+\sum_{i=1}^{4}\beta_i x_i+\sum_{i=1}^{3}\sum_{j=2}^{4}\beta_{ij}x_i x_j+\sum_{i=1}^{2}\sum_{j=2}^{3}\sum_{k=3}^{4}\beta_{ijk}x_i x_j x_k+\beta_{1234}x_1x_2x_3x_4, i<j<k \tag{1}$$

$$x_i=\frac{z_i-\left[z_{i,L}+\frac{1}{2}\times\left(z_{i,H}-z_{i,L}\right)\right]}{z_{i,H}-\left[z_{i,L}+\frac{1}{2}\times\left(z_{i,H}-z_{i,L}\right)\right]}, i=1,\ldots,4 \tag{2}$$

in which z_i is the corresponding experimental variables in real units. $z_{i,\mathrm{L}}$ and $z_{i,\mathrm{H}}$ represent the selected low and high experimental values expressed in real units of the experimental variable $i=1,\ldots,4$. On the basis of the design matrix $\mathbf{D}_{\mathrm{FFD}}$, a model matrix $\mathbf{M}_{\mathrm{FFD}}$ was created according to Equation (3).

$$\mathbf{M}_{\mathrm{FFD}}=[\mathbf{1}\,\overbrace{x_1x_2x_3x_4}^{\mathbf{D}_{\mathrm{FFD}}}\,x_1x_2x_1x_3x_1x_4x_2x_3x_2x_4\cdots x_3x_4x_1x_2x_3x_1x_2x_4x_1x_3x_4 4x_2x_3x_4 4x_1x_2x_3x_4 4] \tag{3}$$

Using the model matrix $\mathbf{M}_{\mathrm{FFD}}$, one can estimate the model parameters that describe the correlation between the experimental variables and their various interaction terms and the outcome of the two distinct products **2b** and **3b**: $y_j^{\mathrm{L}}=f(x_{1,\ldots,}x_4)$, $j\in[3, 5]$, L∈[**L3**, **L4**, **L6**], where the model terms are outlined in Equation (1). By means of gas chromatographic analyses, the responses ($y_1,\ldots,y_5$) were measured for each experiment. The numerical values for the responses y_3 and y_5, yield of **2b** and **3b**, respectively, were multivariate correlated with the model matrix $\mathbf{M}_{\mathrm{FFD}}$ of Equation (3). The numerical values of the regression coefficients were calculated (listed in Table 4) by a multiple linear regression (MLR)[15] method by means of the computer software SAS[21] and MATLAB.[22] The stem plot of Figure 5 shows the experiments that were carried out at low (−1), center (0), and high (+1) settings of the experimental variables. It is evident from Figure 5 that the three distinct catalytic systems involving the ligands **L3**, **L4**, and **L6** operated for the hydrodeiodination. However, the catalytic system comprising the **L3** ligand displayed a pronounced property, it was ca-

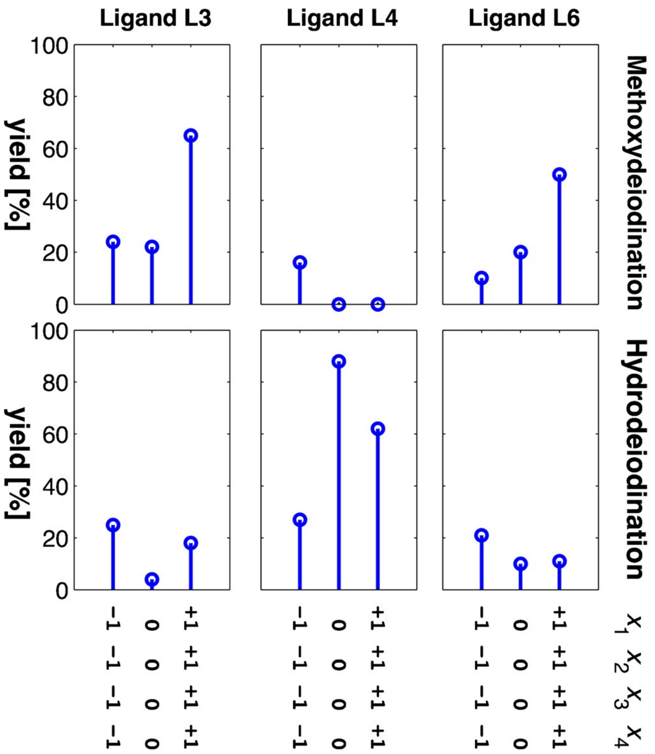

Figure 5. Screening of experimental conditions and three various ligands. Each ligand is explored at three various experimental levels. The form of the responses going from: "all at low level" via "all at center level", to "all at high level" indicates that some of the experimental variables influence the response with quadratic terms. The experimental variables x_k (definition [unit]), levels [−1, 0, +1]: x_1 (reaction temperature [°C]), [90, 100, 110], x_2 (volume of cosolvent [mL]), [0.10, 1.00, 1.90], x_3 (volume of solvent [mL]), [2.00, 2.50, 3.00], x_4 (quantity of base [equiv.]), [0.1, 0.3, 0.5].

Table 3. Experimental results (responses) from a statistical experimental design involving the three ligands **L3**, **L4**, and **L6** as ligands in the Pd-catalyzed two-way switchable process that follows either a hydrodeiodination mechanism or a methoxydeiodination mechanism.

Entry	Experimental variables[a]				Responses[b]														
					L3					**L4**					**L6**				
	x_1	x_2	x_3	x_4	y_1	y_2	y_3	y_4	y_5	y_1	y_2	y_3	y_4	y_5	y_1	y_2	y_3	y_4	y_5
1	−1	−1	−1	−1	25	100	25	100	24	43	63	27	37	16	31	69	21	31	10
2	+1	−1	−1	−1	83	43	36	58	49	100	100	100	0	0	100	100	100	0.1	0.1
3	−1	+1	−1	−1	3	0	0	100	3	46	96	44	4	2	5	100	5	0	0
4	+1	+1	−1	−1	30	24	7	76	23	100	100	100	0	0	100	100	100	0.1	0.1
5	−1	−1	+1	−1	28	0	0	100	28	47	83	39	17	8	27	34	9	66	18
6	+1	−1	+1	−1	80	11	9	89	71	100	100	100	0	0	100	97	97	3	3
6[c]	+1	−1	+1	−1	84	13	11	87	73	–	–	–	–	–	–	–	–	–	–
7	−1	+1	+1	−1	7	0	0	100	7	33	82	27	18	6	14	34	5	66	9
8	+1	+1	+1	−1	78	17	13	83	65	100	100	100	0	0	100	100	100	0.1	0.1
9	−1	−1	−1	+1	17	0	0	39	8	0	0	0	0	0	11	0	0	100	11
10	+1	−1	−1	+1	54	10	5	100	41	81	100	81	0	0	36	42	15	58	21
11	−1	+1	−1	+1	3	0	0	100	3	0	0	0	0	0	0	0	0	0	0
12	+1	+1	−1	+1	22	62	14	38	8	100	100	100	0	0	30	69	21	31	9
13	−1	−1	+1	+1	18	0	0	100	18	0	0	0	0	0	11	0	0	100	11
14	+1	−1	+1	+1	47	5	2	95	45	41	100	41	0	0	73	22	16	68	50
15	−1	+1	+1	+1	9	0	0	100	9	33	100	33	0	0	37	100	37	0	0
16	+1	+1	+1	+1	52	50	4	39	22	88	100	88	0	0	30	34	10	66	20
17	0	0	0	0	83	22	18	78	65	62	100	62	0	0	61	18	11	82	50
18	0	0	0	0	79	21	17	79	62	49	100	49	0	0	49	20	10	80	39
19	−0.5	0	0	0	33	4	1	96	32	–	–	–	–	–	–	–	–	–	–
20	+0.5	0	0	0	77	17	13	83	64	–	–	–	–	–	–	–	–	–	–
21	0	−0.5	0	0	83	12	10	88	73	–	–	–	–	–	–	–	–	–	–
22	0	+0.5	0	0	65	17	11	83	54	–	–	–	–	–	–	–	–	–	–
23	0	0	−0.5	0	74	15	11	85	63	–	–	–	–	–	–	–	–	–	–
24	0	0	+0.5	0	69	17	12	83	57	–	–	–	–	–	–	–	–	–	–
25	0	0	0	−0.5	38	0	0	100	38	–	–	–	–	–	–	–	–	–	–
26	0	0	0	+0.5	88	7	6	93	82	–	–	–	–	–	–	–	–	–	–

[a] Experimental variables x_k (Definition [unit]), levels [−1, 0, +1]: x_1 (reaction temperature [°C]), [90, 100, 110], x_2 (volume of co-solvent [mL]), [0.10, 1.00, 1.90], x_3 (volume of solvent [mL]), [2.00, 2.50, 3.00], x_4 (quantity of base [equiv.]), [0.1, 0.3, 0.5]. [b] y_1 = conversion based on starting material **1b**, y_2 = selectivity towards the hydrodeiodination product **2b**, y_3 = yield of the hydrodeiodination product **2b**, y_4 = selectivity towards the product **3b**, y_5 = yield of methoxydeionination product. All responses were measured by means of GC-MS. [c] Replicate of experiment 6, the experiment that provided the highest outcome in the factorial experimental design part. This experiment was repeated a third time, but the base was added as a solution with the identical quantity to provide quantitative yield of methoxydeiodinated product.

Table 4. Linear models describing the influence of the various experimental variables $x_1,\ldots,x_4$ on the responses y_3 and y_5 studied with three various catalytic systems involving the ligands **L3**, **L4**, and **L6**.

	y_3^{L3}	y_5^{L3}	y_3^{L4}	y_5^{L4}	y_3^{L6}	y_5^{L6}
β_0	8.3333	30.6111	55.0556	1.7778	30.9444	13.9611
β_1	4.0625	14.0000	33.7500	−2.0000	23.8750	2.7688
β_2	−2.4375	−9.0000	6.5000	−1.0000	1.2500	−5.3687
β_3	−3.6875	6.6250	−1.5000	−0.2500	0.7500	3.7438
β_4	−4.0625	−7.2500	−12.1250	−2.0000	−21.1250	5.1062
β_{12}	0.6875	−2.0000	1.7500	1.0000	−0.8750	−0.2438
β_{13}	−0.5625	3.6250	−5.0000	0.2500	−2.3750	1.6187
β_{14}	−0.9375	−4.2500	0.8750	2.0000	−20.7500	6.9813
β_{23}	3.1875	1.6250	2.0000	0.7500	2.5000	−1.2438
β_{24}	3.8125	0.2500	5.8750	1.0000	3.3750	−2.6312
β_{34}	2.0625	−2.3750	−0.8750	0.2500	2.6250	1.2562
β_{123}	0.0625	2.1250	1.5000	−0.7500	−3.6250	−1.3687
β_{124}	0.6875	−3.2500	2.3750	−1.0000	−3.7500	−2.2562
β_{134}	−1.0625	−3.3750	−5.6250	−0.2500	−3.5000	3.3812
β_{234}	−4.0625	−0.8750	5.6250	−0.7500	0.6250	−1.0062
β_{1234}	−0.9375	−0.3750	−2.1250	0.7500	−2.5000	−0.8813
R^2	0.896	0.745	0.996	0.977	0.963	0.540
R^2_{Adj}	0.117	−1.171	0.970	0.801	0.685	−2.912
RMSEP	3.245	11.639	2.172	0.629	7.230	10.952
RSD	3.442	12.345	2.304	0.667	7.669	11.616

pable of facilitating both of the two distinct mechanisms, hydrodeiodination and methoxydeiodination.

The two empirical models $y_3^{L3} = f(x_1, x_2, x_3, x_4)$ and $y_5^{L3} g(x_1, x_2, x_3, x_4)$, outlined in Table 4 were used in an attempt to further optimize the outcome of the processes. Unfortunately, the follow-up optimization experiments failed. Figure 5 indicates that the reason may be due to non-modelled quadratic effects.

To describe these non-linear relationships, a more extensive design is required. The experimental $\mathbf{D}_{FFD}$ (Table 3, entries 1–18) was thus extended to incorporate the necessary experiments (Table 3, entries 19–26).

The collection of the experiments (entries 1–26, which form a new design matrix $\mathbf{D}_{CCD}$) constitute a central composite design (CCD)[23] that also allows to estimate the model of Equation (4).

We decided to further investigate the CCD only for the catalytic system involving the **L3** ligand. By means of the scaled experimental variables $x_1,..,x_4$ the model matrix $\mathbf{M}_{CCD}$ was created according to Equation (5). Two empirical models were derived, $y_3^{L3} = f(x_1, x_2, x_3, x_4)$ and $y_5^{L3} g(x_1, x_2, x_3, x_4)$, by using the multiple linear regression (MLR) method. The estimated model parameters are listed in Table 5. The subsequent step involved pruning of non-significant regression parameters, based on the cumulative normal probability (CND)[24] plots of Figure 6. A new regression was then performed by using this model form to obtain the models listed Table 5.

Table 5. Quadratic models describing y_3^{L3} and y_5^{L3}.

	Full model	
	y_3^{L3}	y_5^{L3}
α_0	10.7650	60.1060
α_1	6.6085	14.5450
α_2	0.5733	−9.3030
α_3	−0.6388	6.2424
α_4	−0.3381	−6.2927
α_{12}	2.0600	−2.0000
α_{13}	0.8100	3.6250
α_{14}	−1.6850	−4.2500
α_{23}	3.9400	1.6250
α_{24}	3.6850	0.2500
α_{34}	1.9350	−2.3750
α_{11}	−8.5068	−36.307
α_{22}	5.4932	25.693
α_{33}	9.4932	11.693
α_{44}	−9.3561	−34.778
R^2	0.731	0.871
R^2_{Adj}	0.389	0.706
RMSEP	4.254	10.542
RSD	4.428	10.973

$$y = f(x_1, x_2, x_3, x_4) = \beta_0 + \sum_{i=1}^{4} \beta_i x_i + \sum_{i=1}^{3} \sum_{j=2}^{4} \beta_{ij} x_i x_j + \sum_{i=1}^{4} \beta_i x_i^2 \quad (4)$$

$$\mathbf{M}_{CCD} = [\mathbf{1}\, \overbrace{x_1x_2x_3x_4}^{\mathbf{D}_{CCD}}\, x_1x_2x_1x_3x_1x_4x_2x_3 \cdots x_2x_4x_3x_4x_1x_1x_2x_2x_3x_3x_4x_4] \quad (5)$$

The final models involving the **L3** ligand (Table 5) were used to produce response surfaces in terms of *iso*-contour projection (Figure 7 a,b and 8), which subsequently were used to predict the optimized conditions of y_3^{L3} and y_5^{L3}, respectively.

The derived model describing the methoxydehalogenation (y_5^{L3}) is reasonable from a modelling point of view and could be used to directly predict optimized conditions (optimized conditions can be found within the boundaries of the experimental domain). The model for hydrodeiodination, however, suggested that a high yield might be attained outside the investigated experimental domain. Therefore, we used the model to produce the response surface *iso*-contour projection in the extrapolated region, which is the region defined by the red lines in Figure 7, (the region above and at the right hand side of the red drawn lines in Figure 8). To evaluate the prediction for the extrapolated region, we conducted the experiments indicated by the red circle in Figure 8, which predict $y_{pred} \approx 65\,\%$ yield. The experiment conducted at the accompanying experimental conditions (see Table 6) provided an almost quantitative yield, which shows that the response surface has a significantly steeper ascent in the extrapolated area.

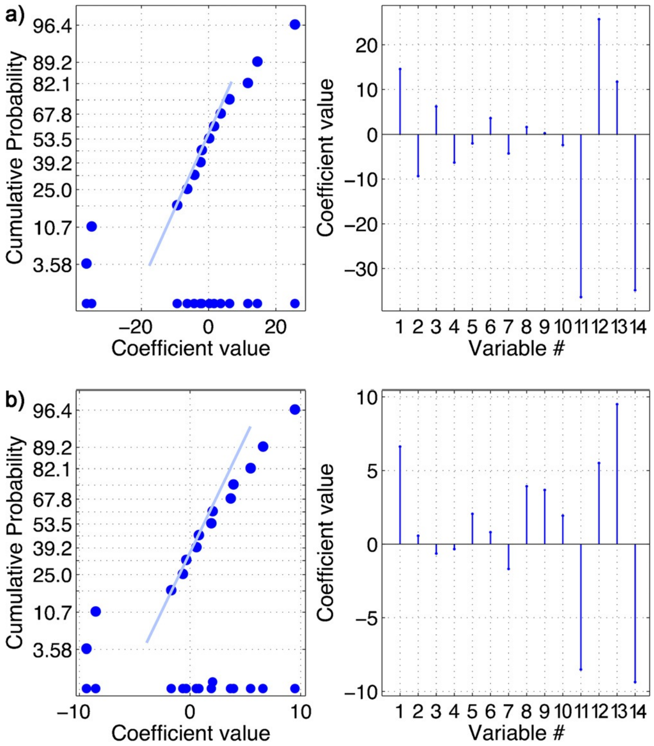

Figure 6. CND plots evaluating the full quadratic models of the a) hydrodeiodination and b) methoxydeiodination pathways.

Scope of the switchable process

A thorough investigation of the scope of the switchable process was performed by investigation of arenes with electron-withdrawing groups. To confirm the findings from above, we also studied some arenes bearing electron-donating groups (Table 7). The hydrodeiodination process proceeded smoothly with electron-withdrawing groups and the method exhibited excellent functional-group tolerance. Carboxylic acid **2j** was hydrodeiodinated smoothly, whereas the reaction with the corresponding *ortho*-substituted carboxylic acid **1i** was unsuccessful. This may be due to formation of a 5-membered palladacycle that includes the carboxylic group. The corresponding *ortho*-substituted carbaldehyde **1m** provided the methoxylated product **2m**. Mixed haloarenes selectively provided the hydrodeiodination product in the presence of a bromine substituent (entry 6) and in one case chloroiodoarene **1g** afforded the hydrodihalogenation product **1h**. Unfortunately, this was

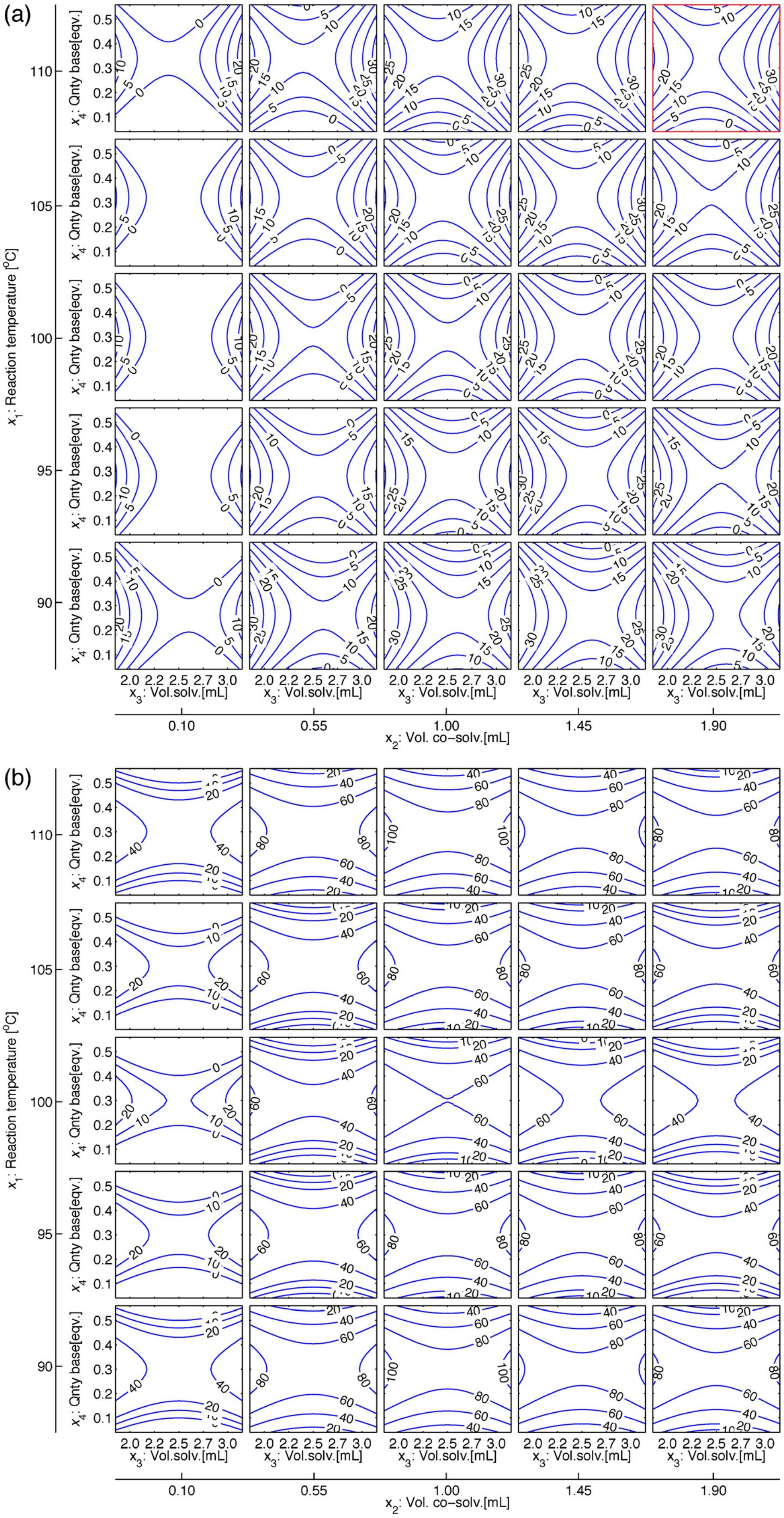

Figure 7. *iso*-Contour projections of the response surfaces (contour lines shows the yield) for the a) hydrodeiodination and b) methoxydeiodination pathways of the two-way switchable Pd-catalyzed process. Each pathway is composed by a plot of a subplot collection that is composed of a 5×5 matrix of 2D *iso*-contour maps. Each of the 2D plots displays the volume of solvent [mL] (x_3) as the abscissa and the quantity of the base [equiv.] (x_4) as ordinate. The locations of the 2D plot in the horizontal direction (the outer frame) view the experimental variable volume of co-solvent [mL] (x_2) at five discrete experimental levels, and in the vertical direction (also at five discrete experimental levels) view the experimental variable x_1, that is reaction temperature [°C].

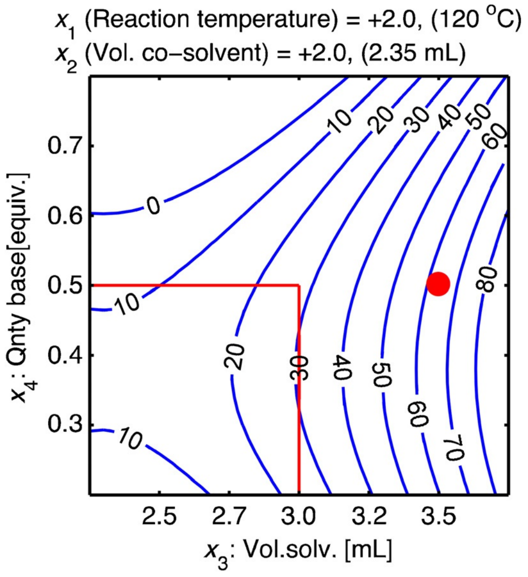

Figure 8. *iso*-Contour projections of the response surface (contour lines show the yield) for the hydrodeiodination pathway of the Pd-catalyzed switchable process. The model predicts higher reaction outcome when the variables x_1, x_2, and x_3 are all extrapolated outside the investigated region (the red lines shows a small part of the experimental domain). The red circle shows the tested experiment, predicted to be $y_{pred}=65\%$.

Table 6. Optimized conditions for the hydrodeiodination and methoxydeiodination reactions

	Experimental value[a]				Pred.[b] [%]	Expe.[b] [%]
	x_1	x_2	x_3	x_4		
y_3[c]	+2	+2	+2	+1	65	100
y_5[c]	+1	−1	+1	−1	100	100

[a] Experimental variables x_k (Definition [unit]), x_1 (reaction temperature [°C]), x_2 (volume of co-solvent [mL]), x_3 (volume of solvent [mL]), x_4 (quantity of base [equiv.]), [b] Pred. = predicted by the model and Expe. = experimental result obtained in experiment. [c] y_3 = yield of the hydrodeiodination product **2b**, y_5 = yield of methoxydeionination product.

a special case, and further experiments showed that other chloroarenes proceeded with only low yields.

Table 7. Scope of the Pd-catalyzed process that follows either a hydrodeiodination mechanism or a methoxydeiodination mechanism.

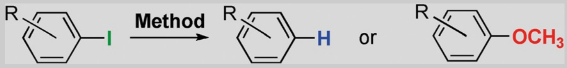

Entry	Iodoarene	Hydrodeiodination[a]	Methoxydehalogenation[a]
1	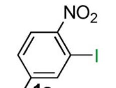 **1a**	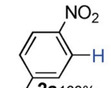 **2a** 100%	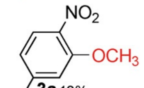 **3a** 13%
2	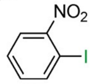 **1b**	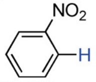 **2b** 100%	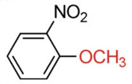 **3b** 100%
3	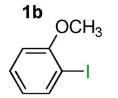 **1c**	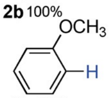 **2c** 13%	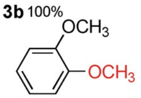 **3c** 0%
4	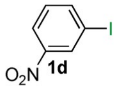 **1d**	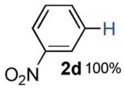 **2d** 100%	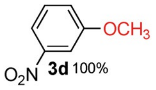 **3d** 100%
5	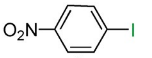 **1e**	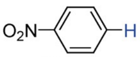 **2e** 100%	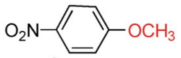 **3e** 100%
6	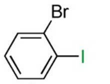 **1f**	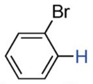 **2f** 43%, 0%[b]	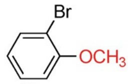 **3f** 0%
7	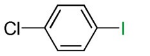 **1g**	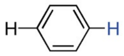 **2g** 100%[c]	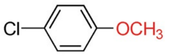 **3g** 0%
8	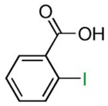 **1i**	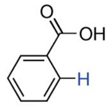 **2i** 0%	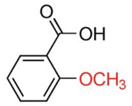 **3i** 0%
9	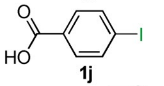 **1j**	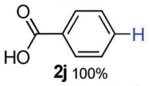 **2j** 100%	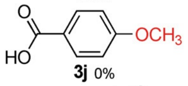 **3j** 0%
10	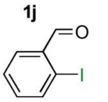 **1m**	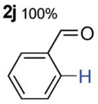 **2m** 64%	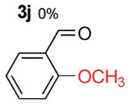 **3m** 40%
11	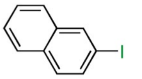 **1o**	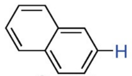 **2o** 51%	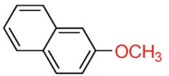 **3o** 51%

[a] Yield based on GC. [b] Reaction time 180 min. [c] Yield based on ^{1}H NMR spectroscopy and checked again authentic samples by GC–MS.

Conclusions

By means of empirical modelling and response surface methodology we were able to establish, develop, and optimize a palladium-catalyzed switchable process that can perform either a hydrodeiodination or a methoxydeiodination reaction. In contrast to commonplace investigations in catalyzed synthesis, which involves the design of dedicated and sophisticated catalysts to achieve high selectivities and yields, we have established a method that involves fine-tuning of the experimental and process variables.

By means of a simple ligand screening we identified the ligand **L3** to be versatile and efficient. By using experimental design and multivariate regression we have established empirical models that describe a two-way switchable process, which allowed us to selectively pursue either hydrodeiodination or methoxydeiodination. Both directions of the process afforded good selectivity and high yields. The hydrodeiodination process operated with electron-withdrawing groups and exhibited excellent functional-group tolerance. The methoxydeiodination process operated well with iodonitrobenzenes.

Experimental Section

General

All chemicals and reagents were purchased from Sigma–Aldrich, Norway (≥97%) and were used without further purification. Distilled and deionized water was used as a cosolvent and solvents (Sigma–Aldrich) were used as reagent-grade quality. The obtained reaction products were compared to authentic samples for identification.

GC–MS analyses were performed on a capillary gas chromatograph equipped with a fused silica column (25 m, 0.20 mm i.d., 0.33 μm film thickness) at a helium pressure of 200 kPa, splitless/split injector and flame ionization detector. ^{1}H NMR spectra were recorded on a NMR spectrometer operating at 400 MHz. ^{13}C NMR spectra were recorded on a NMR spectrometer operating at 150 MHz. Chemical shifts were referenced to the deuterated solvent used in the experiment.

The microwave-assisted experiments were performed by using a Biotage Initiator Sixty EXP Microwave System, which operates at 0–400 W at 2.45 GHz, in the temperature range of 40–250 °C, and a pressure range of 0–20 bar (2 MPa, 290 psi). The reactor-tube volume was 2.5 mL.

Experimental procedure for the screening of solvents, catalysts, and ligands

A microwave reactor tube was charged with 3-nitro-4-iodotoluene (0.19 mmol), catalyst, and ligand (0.15 mol%). The reactor tube was then sealed and carefully flushed with argon through the septa. Degassed solvent (5 mL) and the Pd catalyst was used, a fresh solution of Pd(OAc)$_2$ (0.15 mol%) was added through a syringe. The reactor tube was placed in the microwave cavity and heated at 100 °C for a period of 60 min. The post-reaction mixture was passed through a plug of silica and analyzed by GC–MS. The yield for each experiment can be found in Table 1 in the Supporting Information.

Experimental procedure for base screening

A microwave reactor tube was charged with 3-nitro-4-iodotoluene (0.19 mmol), XPhos-ligand (0.15 mol%) and the base (2 equiv.). The tube was sealed and flushed with argon through the septa. Degassed solvent was then added (5 mL), followed by a freshly prepared solution in the studied solvent of Pd(OAc)$_2$ (0.15 mol%), by means of a syringe. The reactor tube was placed in the microwave cavity and heated at 100 °C for 90 min. The post-reaction mixture was passed through a plug of silica and analyzed by GC–MS. See Table 2 in the Supporting Information for details.

The effect of a cosolvent

A microwave reactor tube was charged with 3-nitro-4-iodotoluene (0.19 mmol), XPhos-ligand (0.15 mol%), TBAB (3 mol%), and KOH (2 equiv.). The reactor tube was then sealed and flushed with argon through the septa. A mixture of water and methanol (see Figure 1 b for details) was added, followed by a freshly prepared solution of Pd(OAc)$_2$ (0.15 mol%) in methanol through a syringe. The tube was placed in the microwave cavity and heated at 100 °C for 90 min. The post-reaction mixture was passed through a plug of silica and analyzed by GC–MS. For experiments where the amount of water was higher than 70%, the starting material was insoluble and no reaction took place. The results are displayed in Figure 2 b.

The effect of a solid base versus an aqueous solution of base

A microwave reactor tube was charged with nitro-2-iodobenzene (0.19 mmol), ligand **3** (5 mol%), TBAB (3 mol%), and KOH (0.5 equiv.). KOH was added either as 1) solid, followed by water (0.1 mL) and methanol (3 mL); or 2) as a solution followed by methanol (3 mL). In both cases, a freshly prepared solution of Pd(OAc)$_2$ in methanol (0.15 mol%) was added through a syringe. The reactor tube was placed in the microwave cavity and heated at 110 °C for 90 min. The post-reaction mixture was passed through a plug of silica and analyzed by GC–MS. The results are displayed in Figure 3.

The effect of the ligand

A microwave reactor tube was charged with either nitro-2-iodobenzene (0.19 mmol) or 2-iodoanisole (0.19 mmol), TBAB (3 mol%), KOH (2 equiv.), and the appropriate ligand (5 mol%). Ligand series are displayed in Figure 2. The reactor tube was sealed and flushed with argon through the septa. A mixture of water and methanol (1:4, 5 mL) was then added. A freshly prepared solution of Pd(OAc)$_2$ (0.15 mol%) in methanol was added through a syringe. The tube was placed in the microwave cavity and heated at 100 °C for a period of 90 min. The post-reaction mixture was passed through a plug of silica and analyzed by GC–MS. The results are displayed in Table 1 and 2.

Procedure for experiments utilized in the experimental design

A microwave reactor tube was charged with nitro-2-iodobenzene (0.19 mmol), TBAB (3 mol%), KOH (0.1–0.5 equiv.), and one of the ligands **3**, **4**, or **6** (5 mol%), before the reactor tube was sealed and flushed with argon through the septa. Water (0.1–1.9 mL) and methanol (2–3 mL) were added through a syringe, followed by a freshly prepared solution of Pd(OAc)$_2$ (0.15 mol%) in methanol. The tube was placed in the microwave cavity and heated at 90–110 °C, for 90 min. The post-reaction mixture was passed through a plug of silica and analyzed by GC–MS. The design matrix containing the setting of each single experiment is displayed in Table 3.

Optimized procedure for the methoxydeiodination reaction

A microwave reactor tube was charged with nitro-2-iodobenzene (0.19 mmol), ligand **3** (5 mol%), and TBAB (3 mol%). Fresh solutions of KOH (0.1 equiv., 0.1 mL) in water and Pd(OAc)$_2$ (0.15 mol%) in methanol were added through a syringe, followed by methanol (3.0 mL). The tube was placed in the microwave cavity and heated at 110 °C for 90 min. The post-reaction mixture was passed through a plug of silica and analyzed by GC–MS, see Table 6 for details.

Optimized procedure for the hydrodeiodination reaction

A microwave reactor tube was charged with haloarene (0.19 mmol), ligand **3** (5 mol%), KOH (0.5 equiv.), and TBAB (3 mol%). Methanol (3.5 mL) was added through a syringe, followed by fresh solution of KOH (0.5 equiv.) and a solution of $Pd(OAc)_2$ (0.15 mol%) in methanol. Finally water (2.8 mL) was added. The tube was placed in the microwave cavity and heated to 120 °C for 90 min. The post-reaction mixture was passed through a plug of silica and analyzed by GC–MS, see Table 6 for details.

Acknowledgements

A.H.S. gratefully acknowledges the Department of Chemistry at the University of Bergen for funding his research fellowship.

Keywords: homogenous catalysis · multivariate regression analysis · palladium · reaction mechanisms · statistical experimental design

[1] F. Alonso, I. P. Beletskaya, M. Yus, *Chem. Rev.* **2002**, *102*, 4009–4091.
[2] a) B. Wei, T. S. A. Hor, *J. Mol. Catal. A* **1998**, *132*, 223–229; b) J. Uenishi, R. Kawahama, Y. Shiga, O. Yonemitsu, *Tetrahedron Lett.* **1996**, *37*, 6759–6762; c) P. P. Cellier, J.-F. Spindler, M. Taillefer, H.-J. Cristau, *Tetrahedron Lett.* **2003**, *44*, 7191–7195; d) C. Amorim, X. Wang, M. A. Keane, *Chin. J. Catal.* **2011**, *32*, 746–755; e) T. Hennebel, J. Benner, P. Clauwaert, L. Vanhaecke, P. Aelterman, R. Callebaut, N. Boon, W. Verstraete, *Biotechnol. Lett.* **2011**, *33*, 89–95; f) A. Pyo, S. Kim, M. R. Kumar, A. Byeun, M. S. Eomb, M. S. Han, S. Lee, *Tetrahedron Lett.* **2013**, *54*, 5207–5210; g) G. Chelucci, S. Figus, *J. Mol. Catal. A* **2014**, *393*, 191–209; h) G. Chelucci, *Chem. Commun.* **2014**, *50*, 4069–4072.
[3] For example, see: a) C. A. Marques, M. Selva, P. Tundo, *J. Org. Chem.* **1993**, *58*, 5256–5260; b) G. V. Lowry, M. Reinhard, *Environ. Sci. Technol.* **1999**, *33*, 1905–1910; c) M. S. Viciu, G. A. Grasa, S. P. Nolan, *Organometallics* **2001**, *20*, 3607–3612; d) J. Moon, S. Lee, *J. Organomet. Chem.* **2009**, *694*, 473–477; e) K. A. Cannon, M. E. Geuther, C. K. Kelly, S. Lin, M. H. R. MacArthur, *Organometallics* **2011**, *30*, 4067–4073; f) H. Min, S. Lee, M. Park, J. Hwang, H. M. Jung, S. Lee, *J. Organomet. Chem.* **2014**, *755*, 7–11; g) E. M. Zahran, N. M. Bedford, M. A. Nguyen, Y.-J. Chang, B. S. Guiton, R. R. Naik, L. G. Bachas, M. R. Knecht, *J. Am. Chem. Soc.* **2014**, *136*, 32–35.
[4] a) G. Mann, J. F. Hartwig, *J. Am. Chem. Soc.* **1996**, *118*, 13109–13110; b) A. V. Vorogushin, X. Huang, S. L. Buchwald, *J. Am. Chem. Soc.* **2005**, *127*, 8146–8149.
[5] a) J. A. Zoltewicz, T. M. Oestreich, A. A. Sale, *J. Am. Chem. Soc.* **1975**, *97*, 5889–5896; b) A. G. Osborne, L. A. D. Miller, *J. Chem. Soc. Perkin Trans. 1* **1993**, 181–184.
[6] M. A. Keegstra, L. Brandsma, *Recl. Trav. Chim. Pays-Bas* **1991**, *110*, 299–300.
[7] J. Lindley, *Tetrahedron* **1984**, *40*, 1433–1456.
[8] S. V. Ley, A. W. Thomas, *Angew. Chem. Int. Ed.* **2003**, *42*, 5400–5449; *Angew. Chem.* **2003**, *115*, 5558–5607.
[9] a) K. E. Torraca, X. Huang, C. Parrish, S. L. Buchwald, *J. Am. Chem. Soc.* **2001**, *123*, 10770–10771; b) S. Kuwabe, K. E. Torraca, S. L. Buchwald, *J. Am. Chem. Soc.* **2001**, *123*, 12202–12206.
[10] a) S. Gowrisankar, A. G. Sergeev, P. Anbarasan, A. Spannenberg, H. Neumann, M. Beller, *J. Am. Chem. Soc.* **2010**, *132*, 11592–11598; b) S. Gowrisankar, H. Neumann, M. Beller, *Chem. Eur. J.* **2012**, *18*, 2498–2502.
[11] Z. Ahmadi, J. S. McIndoe, *Chem. Commun.* **2013**, *49*, 11488–11490.
[12] R. Carlson, J. Carlson, *Design and optimizing in organic synthesis, Data-handling in Science and Technology, Vol. 24*, Elsevier, Amsterdam, **2005**, pp. 21–23.
[13] A. H. Sandtorv, H.-R. Bjørsvik, *Adv. Synth. Catal.* **2013**, *355*, 3231–3243.
[14] a) G. E. P. Box, W. G. Hunter, J. S. Hunter, *Statistics for experimenters. An introduction to design, data analysis, and model building*, Wiley, New York, **1978**; b) G. E. P. Box, N. R. Draper, *Empirical model-building and response surfaces*, Wiley, New York, **1987**.
[15] a) N. R. Draper, H. Smith, *Applied Regression Analysis, 3rd ed.*, Wiley, New York, **1998**; b) D. C. Montgomery, E. A. Peck, *Introduction to linear regression analysis*, Wiley, New York, **1982**.
[16] a) I. T. Jolliffe, *Principal Component Analysis, Springer Series on Statistics*, Springer, New York, **2002**; b) E. R. Malinowski, *Factor Analysis in Chemistry, 3rd ed.*, Wiley, New York, **2002**, pp. 1–432.
[17] K. Ishikawa, *Guide to Quality Control, 2nd ed.*, Asian Productivity Organization, Tokyo, **1982**.
[18] a) H.-R. Bjørsvik, U. M. Hansen, R. Carlson, *Acta Chem. Scand.* **1997**, *51*, 733; b) N. Fey, A. G. Orpen, J. N. Harvey, *Coord. Chem. Rev.* **2009**, *253*, 704–722.
[19] A full factorial design (FFD) is a statistical experimental design that is constituted by all possible combinations of a set of experimental variables (factors). FFD is the most fool-proof design approach that supports both continuous variables (e.g. reaction temperature, concentration, etc.) and categorical variables (type of catalyst, base, etc.). In FFD, an experimental run is conducted at every combination of the selected experimental level. The number of experiments (in the design matrix **D**) is determined by the number of experimental levels and variables. For example, a full factorial design composed of three variables ($k=3$) that is investigated at two experimental levels, requires $2^k=2^3=8$ experiments. In addition, some experiments (c) in the center of the experimental design are included.
[20] Standard order of a design matrix **D** for a full factorial design with k variables at two experimental levels is created in the following way. The first (x_1) column of the **D** matrix starts with -1 and alternates in sign for all 2^k runs. The second (x_2) column starts with -1 repeated two times, and then two repeats of $+1$ until all 2^k places are filled for column (x_2). The third column (x_3) starts with -1 that is repeated four times, then four repeats of $+1$ and so on. General: x_i, $i=1,\dots,k$ (variables - columns) starts with 2^{i-1} repeats of -1 followed by 2^{i-1} repeats of $+1$.
[21] For example, see: a) *Base SAS 9.2 Procedures Guide*, N. C. Cary, SAS Institute Inc, **2009**; b) *SAS/GRAPH 9.2: Statistical Graphics Procedures Guide, 2nd ed.*, N. C. Cary, SAS Institute Inc. **2010**.
[22] For example, see: a) *Using MATLAB, version 6*, The Matwork, Inc., M. A. Natick, **2000**; b) *Using MATLAB Graphics, version 6*, The Matwork, Inc., M. A. Natick, **2000**; c) D. Hanselman, B. Littlefield, *Mastering MATLAB: A Comprehensive Tutorial and Reference*, Prentice-Hall Inc., Upper Saddle River, NJ, **1996**.
[23] A central composite design (CCD) is composed by a factorial design including some center experiments and a group of star points (star design). The composite design allows the calculation of model parameters that can account for the curvature of a response surface. Although the distance from the center (0) of the factorial design point is ± 1 (scaled units) for each variable (factor), the distance from the center to a star point possess a value of $|\alpha| \neq 1$. CCDs make use of in total five experimental levels, namely ± 1, $\pm\alpha$, and 0 (scaled units). The CCD used herein is composed by $(2^k+2k+c,\ k=4,\ c=2)=26$ experiments.
[24] The cumulative normal probability (CND) plot is a graphical tool that can be used to evaluate whether or not a data vector is nearly statistically normal distributed. The data vector are plotted against a theoretical normal distribution in such a way that the data points should form an approximate straight line. Departures from this straight line indicate departures from normality. Thus, when the vector of regression coefficients is evaluated in a CND plot, the data point that follows the straight line will be non-significant coefficients (normal distributed noise). The data point that falls off-line represent significant contributing models terms and should thus be included in the final model. See: a) C. Daniel, *Technometrics* **1959**, *1*, 311–341; b) A. Birnbauma, *Technometrics* **1959**, *1*, 343–357.

Received: March 5, 2015